analytical chemistry

ACS Editors' Choice

Article

pubs.acs.org/ac

Terms of Use

Inside Amber: The Structural Role of Succinic Acid in Class Ia and Class Id Resinite

Jennifer Poulin* and Kate Helwig

Canadian Conservation Institute, 1030 Innes Road, Ottawa, Ontario Canada, K1B 4S7

ABSTRACT: For the first time, molecular evidence of the structural role played by succinic acid within the macromolecular structure of Class Ia and Class Id resinite is presented. Using a novel gas chromatographic methodology, communol (Class Ia) and ozol (Class Id) moieties within the polylabdane matrix are shown to be cross-linked with succinic acid. Samples were analyzed using pyrolysis-gas chromatography−mass spectrometry with in situ hexamethyldisilazane derivatization, using a thermal separation probe to perform the pyrolysis and sample introduction. The relatively slow rate of heating and prolonged pyrolysis of resinites using this new methodology, combined with the use of a mild derivatization reagent, allowed communol pyrolysates from Class Ia resinite and ozol pyrolysates from Class Id resinite to elute with unbroken succinyl ester cross-linkages. These results provide direct molecular evidence that the key role of succinic acid within Class Ia and Class Id resinite is to cross-link the macromolecular structure. In the Class Id resinite, the methodology also allowed the detection of succinyl ester linkages between ozol pyrolysates and dehydroabietol, thus demonstrating that nonpolymerized diterpenes contribute structurally to the macromolecular structure of Class Id resinite.

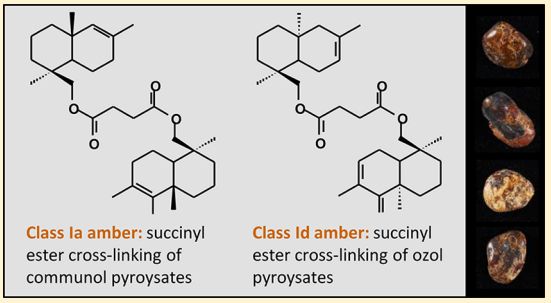

Amber (resinite) is formed through the natural polymerization and fossilization of exuded plant resin over the course of millions of years. Although produced from many different plant species, distinctions in chemical composition have allowed resinite from different deposit sites to be distinguished, and, in some cases, allowed the determination of plant origins.[1−7] Of the numerous resinites analyzed and classified to date, the most common are described by Class I, having macromolecular structures based on polymers of labdanoid diterpenes.[2] Presently, the following four subcategories of Class I resinites have been defined:[8−10]

Class Ia: resinites based on labdanoid diterpenes having a regular configuration, including communic acid, communol, and biformenes, and incorporating succinic acid. Baltic resinite is the only Class Ia resin to date.

Class Ib: resinites based on labdanoid diterpenes having a regular configuration, including communic acid, communol, and biformenes, with the absence of succinic acid. This subclass is the most common throughout the world.

Class Ic: resinites based on labdanoid diterpenes having an enantio configuration, including ozic acid, ozol, and enantio biformenes, with the absence of succinic acid.

Class Id: resinites based on labdanoid diterpenes having the enantio configuration, including ozic acid, ozol, and enantio biformenes and incorporating significant amounts of succinic acid. To date, Class Id resinites have been found only in Canada.

The polylabdanoid matrix of Class I resinites is extremely durable. Although this very quality ensured that it would withstand millions of years of environmental exposure, and survive to be analyzed in the modern day, it also means that chromatographic analysis cannot be completed through extraction alone. Because the polylabdane matrix is insoluble and resistant to chemical breakdown, pyrolysis-gas chromatography−mass spectrometry (Py-GC−MS) is required to identify the monomer units. As resinite is pyrolyzed, the macromolecular structure is broken apart. Monomer labdanoid units within the natural polymer are separated and additional materials that have been captured within the matrix are also released, including nonpolymerizable, intact diterpene compounds and succinic acid. Currently there are two subclasses of Class I resinite that contain a high proportion of succinic acid, Baltic resinite (Class Ia) and certain resinites from Canada (Class Id). The succinic acid in these resinites is believed to cross-link the polymer matrix through esterification to the communol moieties in Class Ia resinites and the ozol moieties in Class Id resinites.[10−14] Although cross-linking through esterification has been hypothesized, to date, no intact dicommunyl succinate esters or diozyl succinate esters have been identified using Py-GC−MS analysis techniques; under the optimized pyrolysis conditions, these linkages seem to fragment, yielding separate communol pyrolysates and succinic acid.[8] In a previous report on the Py-GC−MS analysis of Class Id resinite from Axel Heiberg, however, Anderson and LePage tentatively identified two compounds consisting of ozol pyrolysates esterified to methylated succinic acid.[2] Although not showing complete cross-linking of labdane alcohol moieties within the macromolecular structure, this was a step toward

Received: March 25, 2014
Accepted: June 19, 2014
Published: June 19, 2014

 © 2014 American Chemical Society dx.doi.org/10.1021/ac501073k | *Anal. Chem.* 2014, 86, 7428−7435

verifying the hypothesis. The results reported here, using a thermal separation probe (TSP) to perform the pyrolysis and sample introduction, show direct molecular evidence of the cross-linking for the first time. The new methodology also shows that dehydroabietol, a major nonpolymerized diterpene in Class Id resinite,[2,10] is linked through succinic acid to the macromolecular structure and not simply occluded within the matrix.

Previous studies using Py-GC–MS have utilized flash pyrolysis at the optimized temperature of 480 °C, sustained for only a few seconds before cooling quickly back down to ambient temperature.[1,2,8–10,14–16] The methodology using a TSP reported here uses a slightly lower pyrolysis temperature (450 °C), a slower heating rate (900 °C/min), and an extended isothermal dwell time (the final temperature was held for 3 min and then slowly decreased to 250 °C). It is these changes that effectively altered what had in the past been an immediate pyrolysis, to a slower one. These seemingly minor variations make a substantial difference in the size and complexity of compounds that are released from the rigid polymer matrix. As in previous work, hexamethyldisilazane (HMDS) was chosen for the in situ derivatization as it provides a milder alternative to tetramethylammonium hydroxide (TMAH) in the analysis of natural resins.[10,17–22]

EXPERIMENTAL SECTION

Resinite Samples. Three different Class Ia Baltic resinite samples (from the Canadian Museum of Nature and a private collection) and four Class Id Canadian resinite samples (from the Canadian Conservation Institute, the Royal Ontario Museum, and the Canadian Museum of Nature) were studied. Similar results were obtained within the two classes, and one from each is presented. The Class Id resinite described in this paper dates from the Eocene.[23] The sample was collected by R. Day in 1988 from level K of the Fossil Forest hill and it consists of ovular balls ranging in approximate size from 5–30 mm in length.[24] The outer surfaces of the resin balls are brittle, granular, and weathered in appearance. The Class Ia resinite presented was collected near the Baltic Sea. This sample was acquired from the F. Ebbutt collection in the Canadian Museum of Nature. It exists as fragments only, not an intact resin ball.

Py(TSP)-GC–MS. Pyrolysis was carried out using a TSP (Agilent Technologies, Inc., Palo Alto, CA) installed in a multimode inlet on an Agilent 7890A GC System gas chromatograph (Agilent Technologies, Inc., Palo Alto, CA), interfaced to a 5975C single quadrapole mass selective detector (Agilent Technologies, Inc., Palo Alto, CA). The MS was operated in EI positive mode (70 eV). The MS transfer line temperature was 280 °C; the MS ion source was kept at 230 °C and the MS quadrapole at 150 °C. The MS was run in scan mode from 50–550 amu (5–25 min), 50–750 amu (25–30 min), and 50–800 amu (35–63 min). For the gas chromatographic separation, a Phenomenex ZB-SemiVolatiles fused silica column (30 m × 0.25 mm i.d., 0.25 μm film thickness; Phenomenex Inc., Torrance, CA) was used. The carrier gas was operated in constant flow mode (He, purity 99.9993%; Linde Canada) at 1.2 mL/min. The multimode injector with TSP was operated in split mode (25:1) and ramped from 50 to 450 °C, at a rate of 900 °C/min. The final temperature was held constant for 3 min and then decreased to 250 °C at a rate of 50 °C/min. The chromatographic oven was programmed from 40 to 200 °C at 10 °C/min and 200 to 310 °C at 5 °C/min with a hold time of 25 min (63 min run time). Data were processed using Agilent ChemStation software (v.E.02.02). In addition to elucidation of mass spectra based on molecular weight and fragmentation, mass spectral identification was also performed using the NIST 11 Mass Spectral Library and published reference data.[14]

In Situ HMDS Derivatization. For each analysis, approximately 50 μg of finely ground resinite was placed in a TSP microvial (Agilent Technologies, part no. 5190-3187) with 2 μL of hexamethyl disilazane (HMDS, Supelco, Bellafonte, PA). The TSP was inserted into the GC inlet held at 50 °C and the run was started remotely using ChemStation software.

Method Repeatability. To determine the repeatability, the pyrolysis methodology described above was carried out with five subsamples of homogeneously ground Class Ia resinite. All of the communol pyrolysate monomers, monosuccinate esters, and disuccinate esters were detected in each subsample. The relative standard deviations (RSD) of the integrated peak area of a representative communol pyrolysate monomer, monoester, and diester were calculated. The RSD of the communol pyrolysate monomer was approximately 5%, while the less abundant monoester and diester pyrolysates were 15% and 20%, respectively.

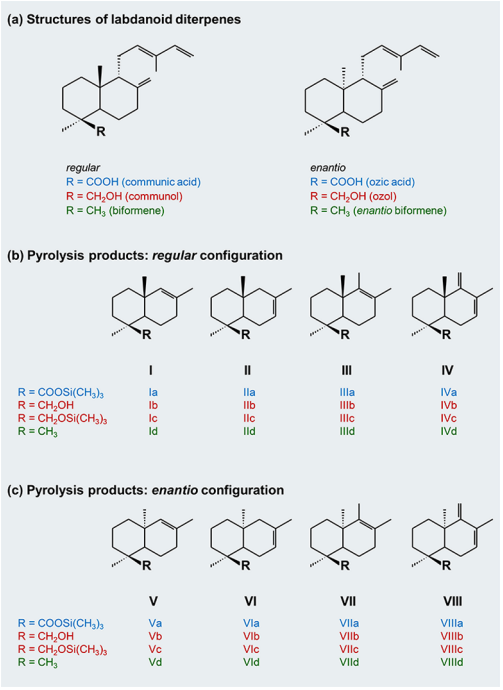

Figure 1. (a) Molecular structures of the regular and enantio labdanoid configurations found in Class I resinites. (b) Molecular structures of compounds with a regular configuration formed through Py(HMDS)-GC–MS. (c) Molecular structures of compounds with an enantio configuration formed through Py(HMDS)-GC–MS. The structures and labels refer to compounds listed in Figures 2–8 and Table 1.

RESULTS AND DISCUSSION

Pyrolysis of Class I Resinite. All Baltic resinite is classified as Class Ia (regular)[16] and the Axel Heiberg resinite in this study has been recently classified as Class Id (enantio).[10] The molecular structures of the components that make up their polymer frameworks are depicted in Figure 1a. The pyrolysis of

dx.doi.org/10.1021/ac501073k | Anal. Chem. 2014, 86, 7428–7435

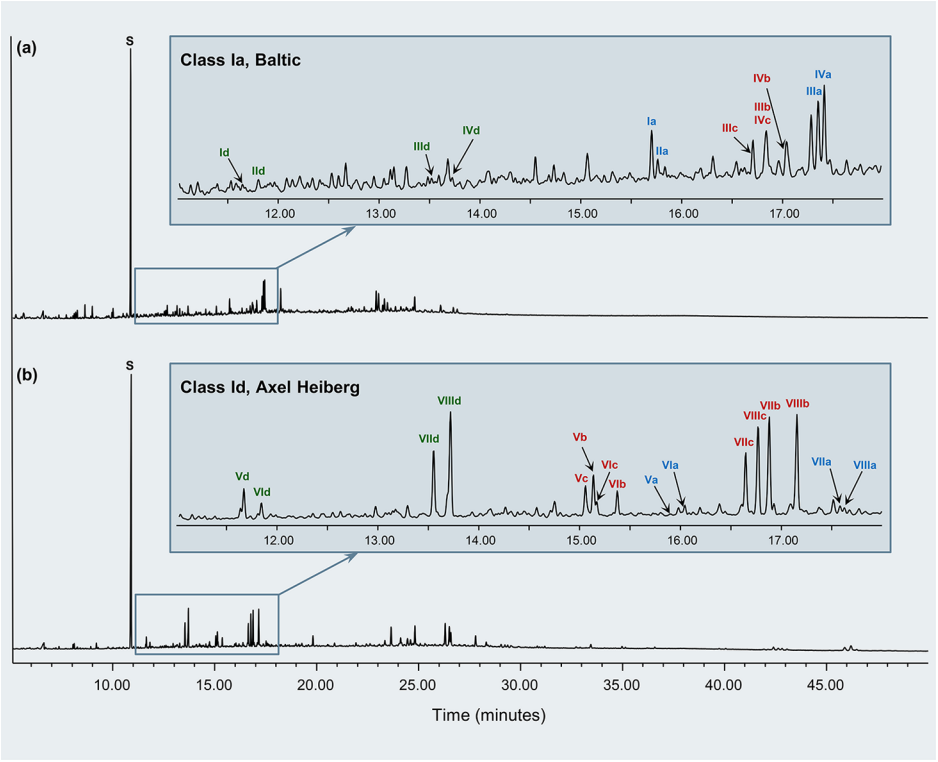

Figure 2. Chromatograms of Class Ia Baltic resinite (a) and Class Id Axel Heiberg resinite (b) with expansion of the segments between 11 and 18 min to show peaks of characteristic pyrolysates of the macromolecular structures. Pyrolysates forming from the labdanoid carboxylic acids are labeled in blue, the alcohol pyrolysates are labeled in red, and the hydrocarbon pyrolysates are labeled in green. The labeled peaks correspond to molecular structures depicted in Figure 1.

all Class I resinites produces characteristic sets of four pyrolysates for the acid, alcohol, and hydrocarbon polymeric constituents. The pyrolysates of Class Ia Baltic resinite include those originating from communic acid, communol, and biformenes (structures I–IV in Figure 1b); whereas the pyrolysates of Class Id resinite from Canada include those originating from ozic acid, ozol, and enantio biformenes (structures V–VIII in Figure 1c). These structurally similar sets of compounds can be separated using gas chromatography and a capillary column of appropriate stationary phase.[15] The labeling of Class I resinite pyrolysis products is often confusing, largely due to the complex nomenclature of the compounds and lack of trivial names. For this reason, the structures in Figure 1 are labeled following a previously published convention.[25,26]

Polylabdanoid Monomers. Chromatograms of ground and homogenized Baltic and Axel Heiberg resinite are depicted in Figure 2a,b. Peaks in the chromatograms are labeled in accordance with Figure 1. The characteristic ion fragments for the peaks are provided in Table 1. The most prominent feature of both chromatograms is the derivatized succinic acid peak (S). The compound is of such significance that its presence warrants separate subclasses for these two types of resinite. The portion of the chromatograms showing the individual polylabdanoid pyrolysates (11–18 min) has been expanded to more clearly resolve the peaks of particular interest.

The regular and enantio polylabdanoid pyrolysates can be differentiated chromatographically because communic acid and ozic acid, and communol and ozol are not actually enantiomers, but rather epimers. However, the terms "regular" and "enantio" are so abundant in the Class I resinite vernacular that they remain in use.[26] As they are epimers, the pyrolysates from communic acid elute at slightly different times than the pyrolysates of ozic acid; and the same is true for communol and ozol. A previous copyrolysis experiment of Class Ia Baltic resinite and Class Id Canadian resinite show this separation between so-called regular and enantio resinites.[10] These staggered elution times are visible in the Figure 2 chromatograms.

From Figure 2, it is clear that there are differences in the relative abundances of acid, alcohol, and hydrocarbon units that make up the macromolecular structures of Class Ia Baltic resinite and Class Id Axel Heiberg resinite. The characteristic sets of pyrolysates (labeled I–IV in Figure 2a and V–VIII in Figure 2b) are produced for both resinites; however, the relative proportions differ significantly. In the Baltic resinite sample (Figure 2a), the pyrolysates from communic acid (Ia–IVa) are the most abundant, followed by those from communol (compounds Ic–IVc) and biformenes (Id–IVd). These results have been previously reported using Py(TMAH)-GC–MS.[14] In contrast, the Axel Heiberg resinite is most abundant in enantio biformenes (Vd–VIIId) and ozol (Vb–VIIIb and Vc–VIIIc), with relatively less ozic acid (Va–VIIIa) incorporated in the polymer.

For both subclasses, in addition to the peaks corresponding to derivatized alcohol pyrolysates, there is also evidence of significant amounts of their underivatized analogues. In the Baltic resinite sample, due to a lower abundance of communol, only the two larger underivatized pyrolysates (IIIb and IVb) are resolved from the baseline and labeled. Whereas, in the Axel Heiberg resinite, which has significantly more ozol, all four underivatized ozol pyrolysates (Vb–VIIIb) are labeled. The

dx.doi.org/10.1021/ac501073k | Anal. Chem. 2014, 86, 7428–7435

Table 1. List of Compounds Corresponding to Marked Peaks in Figures 3, 5, and 7

peak label	pyrolysate*	MW	*m/z* values of characteristic fragment ions (% abundance)
Ib-S	communyl succinate, TMS ester (Ib)	380	175 (100), 190 (86), 95 (67), 173 (62), 73 (44), 147 (16), 380 (4)
IIb-S	communyl succinate, TMS ester (IIb)	380	175 (100), 190 (96), 107 (69), 119 (62), 73 (50), 223 (42), 380 (9)
IIIb-S	communyl succinate, TMS ester (IIIb)	394	189 (100), 109 (83), 173 (80), 204 (63), 119 (57), 73 (53), 394 (11)
IVb-S	communyl succinate, TMS ester (IVb)	392	132 (100), 173 (97), 187 (69), 73 (55), 119 (46), 202 (37), 392 (13)
Vb-S	ozyl succinate, TMS ester (Vb)	380	175 (100), 95 (100), 190 (53), 73 (51), 119 (33), 380 (2)
VIb-S	ozyl succinate, TMS ester (VIb)	380	175 (100), 190 (97), 105 (86), 73 (80), 119 (75), 380 (4)
VIIb-S	ozyl succinate, TMS ester (VIIb)	394	189 (100), 173 (70), 109 (53), 204 (46), 73 (36), 394 (7)
VIIIb-S	ozyl succinate, TMS ester (VIIIb)	392	187 (100), 146 (59), 132 (46), 173 (31), 73 (31), 202 (27), 392 (<1)
Ib-S-Ib	dicommunyl succinate (Ib, Ib)	498	190 (100), 95 (85), 175 (66), 191 (47), 109 (46), 498 (2)
Ib-S-IIb	dicommunyl succinate (Ib, IIb)	498	190 (100), 95 (93), 191 (86), 107 (46), 175 (39), 498 (1)
Ib-S-IIIb	dicommunyl succinate (Ib, IIIb)	512	204 (100), 95 (99), 109 (92), 191 (81), 189 (77), 190 (36), 175 (24),512 (5)
Ib-S-IVb	dicommunyl succinate (Ib, IVb)	510	95 (100), 191 (70), 202 (57), 132 (52), 187 (41), 175 (10), 190 (10), 510 (2)
IIb-S-IIIc	dicommunyl succinate (IIb, IIIb)	512	109 (100), 190 (64), 95 (64), 119 (50), 204 (42), 189 (33), 175 (24), 512 (6)
IIb-S-IVb	dicommunyl succinate (IIb, IVb)	510	95 (100), 202 (83), 119 (80), 132 (72), 187 (59), 190 (43), 175 (27), 510 (5)
IIIb-S-IIIbc	dicommunyl succinate (IIIb, IIIb)	526	109 (100), 204 (60), 189 (56), 205 (56), 95 (42), 119 (32), 526 (1)
IIIb-S-IVb	dicommunyl succinate (IIIb, IVb)	524	109 (100), 205 (43), 95 (36), 202 (36), 187 (28), 189 (18), 204 (12), 524 (3)
IVb-S-IVb	dicommunyl succinate (IVb, IVb)	522	202 (100), 132 (94), 203 (93), 187 (92), 146 (61), 522 (13)
Vb-S-Vb	diozyl succinate (Vb, Vb)	498	190 (100), 175 (89), 95 (80), 205 (19), 161 (16), 498 (3)
Vb-S-VIb	diozyl succinate (Vb, VIb)	498	190 (100), 105 (5), 95 (50), 175 (44), 119 (40), 498 (<1)
VIb-S-VIb	diozyl succinate (VIb, VIb)	498	190 (100), 95 (76), 175 (67), 119 (40), 161 (30), 498 (3)
Vb-S-VIIb	diozyl succinate (Vb, VIIb)	512	189 (100), 95 (95), 205 (68), 109 (63), 204 (60), 175 (50), 190 (44), 512 (<1)
Vb-S-VIIIb	diozyl succinate (Vb, VIIIb)	510	187 (100), 95 (74), 146 (67), 202 (51), 132 (31), 175 (24), 190 (5), 510 (1)
VIb-S-VIIb	diozyl succinate (VIb, VIIb)	512	189 (100), 109 (86), 205 (84), 95 (60), 204 (56), 190 (49), 175 (32), 512 (<1)
VIb-S-VIIIb	diozyl succinate (VIb, VIIIb)	510	187 (100), 146 (68), 202 (51), 95 (39), 132 (37), 175 (16), 190 (10), 510 (<1)
VIIb-S-VIIb	diozyl succinate (VIIb, VIIb)	526	109 (100), 205 (80), 189 (79), 121 (47), 204 (39), 95 (32), 526 (>1)
VIIb-S-VIIIb	diozyl succinate (VIIb, VIIIb)	524	187 (100), 109 (84), 202 (69), 146 (63), 189 (42), 132 (27), 204 (17), 524 (<1)
VIIIb-S-VIIIb	diozyl succinate (VIIIb, VIIIb)	522	187 (100), 133 (60), 203 (58), 146 (58), 202 (52), 107 (46), 119 (42), 522 (<1)
S-DHAol	dehydroabietyl succinate, TMS ester	458	253 (100), 173 (58), 268 (36), 73 (26), 197 (25), 211 (17), 458 (5)
Vb-S-DHAol	dehydroabietyl ozol succinate (Vb)	576	190 (100), 173 (88), 253 (87), 175 (56), 95 (55), 268 (27), 190 (25), 576 (0)
VIb-S-DHAol	dehydroabietyl ozol succinate (VIb)	576	190 (100), 173 (78), 253 (57), 161 (55), 175 (22), 268 (22), 576 (0)
VIIb-S-DHAol	dehydroabietyl ozol succinate (VIIb)	590	189 (100), 173 (94), 204 (85), 253 (46), 109 (43), 133 (34), 268 (9), 590 (0)
VIIIb-S-DHAol	dehydroabietyl ozol succinate (VIIIb)	588	187 (100), 173 (77), 146 (58), 202 (55), 266 (31), 133 (30), 253 (20), 268 (7), 588 (0)

*Communyl and ozyl pyrolysates labeled Ib–VIIIb are described in Figure 1. Compounds are tentatively assigned based on elucidation of mass spectra. Examples of molecular structures of the monoesters and diesters are shown in Figures 4 and 6, respectively.

presence of both derivatized and underivatized labdane alcohol pyrolysates in chromatograms of Class Ia and Class Id resinites has been previously reported.[2,10,14]

Succinic Acid Esterification: Monoesters. In Figure 3a,b, segments of the Class Ia and Class Id chromatograms have been expanded (23.5–28 min) to focus on a region that, in addition to nonpolymerized diterpenes, contains a series of significant peaks related to the macromolecular structure. In each chromatogram, the labeled peaks are polylabdanoid alcohol pyrolysates esterified to trimethylsilylated succinic acid. The possibility of cross-linking communol monomer units by succinic acid in the macromolecular structure of Class Ia resinite was postulated by Gough and Mills in 1972.[11] The Fourier transform infrared (FTIR) spectra of both Class Ia and Class Id resinites supports this hypothesis with strong ester bands at approximately 1735 and 1160 cm^{-1}.[10,13,27] Although the FTIR spectra provide evidence that esterification has taken place, the precise compounds that form the esters cannot be determined by this technique alone.

For both the Class Ia resinite and the Class Id resinites, these succinlyated pyrolysate compounds elute as two sets of pairs. This can also be seen for the characteristic bicyclic acid, alcohol and hydrocarbon monomer pyrolysates in Figure 2. This distinctive pattern is useful in identifying unknown compounds related to the pyrolysates. In addition, the compounds in Figure 3 were unambiguously identified by fragmentation patterns and molecular ions in their mass spectra. Key fragmentations and characteristic ions for the monoesters are provided in Figure 4 and Table 1. The *m/z* 73 ion is indicative of trimethylsilyl derivatization. The ions of highest mass in the mass spectra at *m/z* 380 (Ib-S, IIb-S, Vb-S, and VIb-S), *m/z* 394 (IIIb-S and VIIb-S), and *m/z* 392 (IVb-S) were attributed to the molecular ions ($M^{+\bullet}$). The $M^{+\bullet}$ for compound VIIIb-S was not present; however, the ion at *m/z* 377 was present, indicating loss of a methyl group $[M\text{-}15]^+$. Characteristic fragment ions include *m/z* 175 and *m/z* 190 for compounds Ib-S, IIb-S, Vb-S, and VIb-S; *m/z* 189 and *m/z* 204 for compounds IIIb-S and VIIb-S; *m/z* 187 and *m/z* 202 for compounds IVb-S and VIIIb-S. These fragment ions are presumed to be formed through elimination of the methyl group at the junction of the A/B rings followed by dehydrogenation and cleavage of the C–O bond at the succinate group (Figure 4). Similar reaction pathways have been studied for analogous oxygenated aromatic diterpenes.[28] These ions are also found in the mass spectra of the earlier-eluting trimethylsilylated pyrolysates in Figure 2, which have been previously published.[10]

Just as the retention times for the sets of four nonesterified pyrolysates from communol and ozol are staggered in Figure 2a,b, with the enantio compounds Vc–VIIIc eluting slightly faster than their regular counterparts (Ic–IVc), so too are the

dx.doi.org/10.1021/ac501073k | Anal. Chem. 2014, 86, 7428–7435

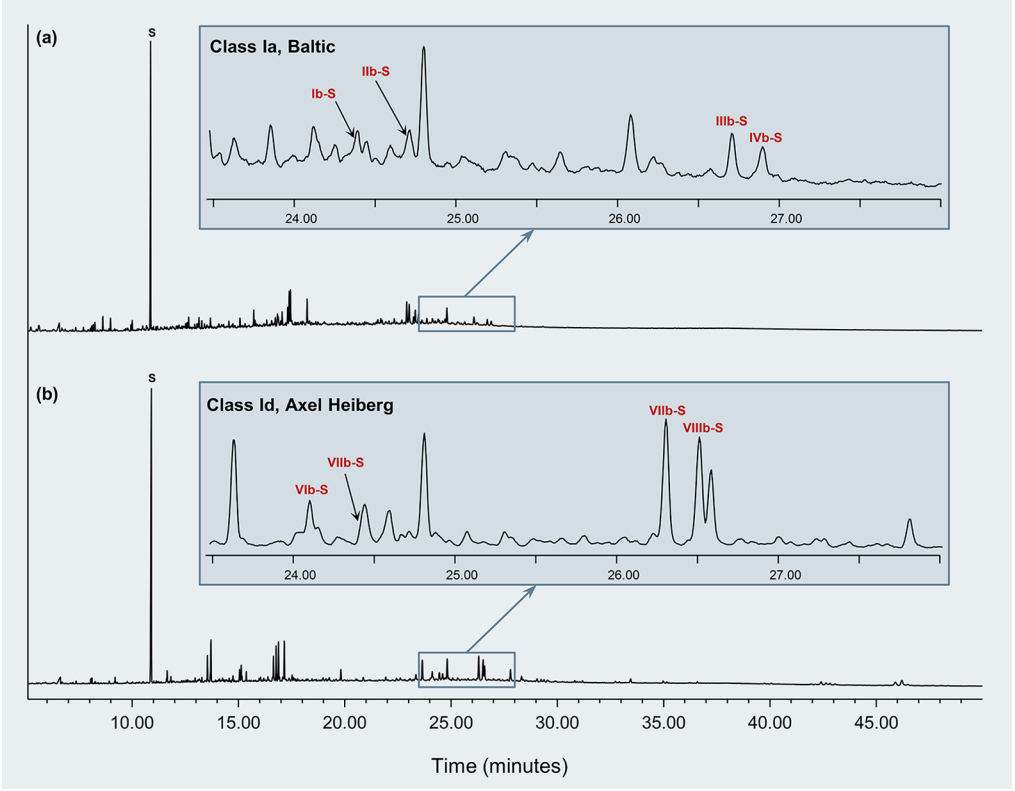

Figure 3. Chromatograms of Class Ia Baltic resinite (a) and Class Id Axel Heiberg resinite (b) with expansion of the segments between 23.5 and 28 min to show peaks of the esterification of trimethylsilylated communyl and ozyl succinate pyrolysates, respectively. The labeled peaks correspond to structures described in Figure 4 and mass spectra in Table 1.

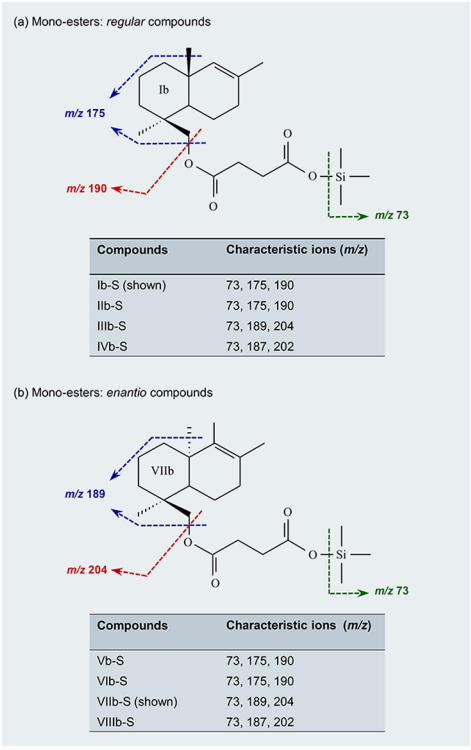

Compounds	Characteristic ions (*m/z*)
Ib-S (shown)	73, 175, 190
IIb-S	73, 175, 190
IIIb-S	73, 189, 204
IVb-S	73, 187, 202

Compounds	Characteristic ions (*m/z*)
Vb-S	73, 175, 190
VIb-S	73, 175, 190
VIIb-S (shown)	73, 189, 204
VIIIb-S	73, 187, 202

Figure 4. Key fragmentations and resulting ions of the monoester compounds for the Class Ia resinite (a) and Class Id resinite (b).

retention times for the esterified pyrolysates in Figure 3a,b. The macromolecular structure of the Class Ia Baltic resinite sample contains a relatively low abundance of communol (Figure 2a).[14] Thus, it is reasonable that the peaks for these succinylated communol compounds (Ib-S to IVb-S, Figure 3a) are also relatively small. In contrast, the esterified ozol pyrolysate peaks (Vb-S to VIIIb-S, Figure 3b) are relatively abundant, corresponding to a greater abundance of ozol in the macromolecular structure of the Axel Heiberg resinite (Figure 2b).[10] The succinic acid in these compounds is only esterified with alcohol polylabdanoid pyrolysates on one of the carboxylic acid groups and thus does not illustrate full cross-linking through the succinic acid.

Succinic Acid Esterification: Diesters. In Figure 5a,b, segments of the Class Ia and Class Id chromatograms have been expanded (39−50 min) to highlight the fully esterified succinate compounds for Class Ia and Class Id resinite, respectively. As seen in Figures 1 and 2, during pyrolysis, alcohol polylabdanoid diterpenes form four characteristic bicyclic compounds. For Class Ia resinite, there are 10 different permutations that can arise from the esterification of a molecule of succinic acid with any two of the four characteristic bicyclic compounds. The same holds true for Class Id resinite. These combinations correspond to the labeled peaks in each chromatogram. In Figure 5a, the first cluster of peaks consists of three succinate diesters formed from the relatively less abundant compounds Ib and IIb, and the peaks are quite small. The central cluster of peaks also contains succinate diesters containing compounds Ib and IIb, but in combination with the relatively more abundant compounds IIIb and IVb. These peaks are larger and better resolved from the baseline than the first set. The final cluster of peaks are succinate diesters formed from only the more abundant compounds IIIb and IVb and

dx.doi.org/10.1021/ac501073k | *Anal. Chem.* 2014, 86, 7428−7435

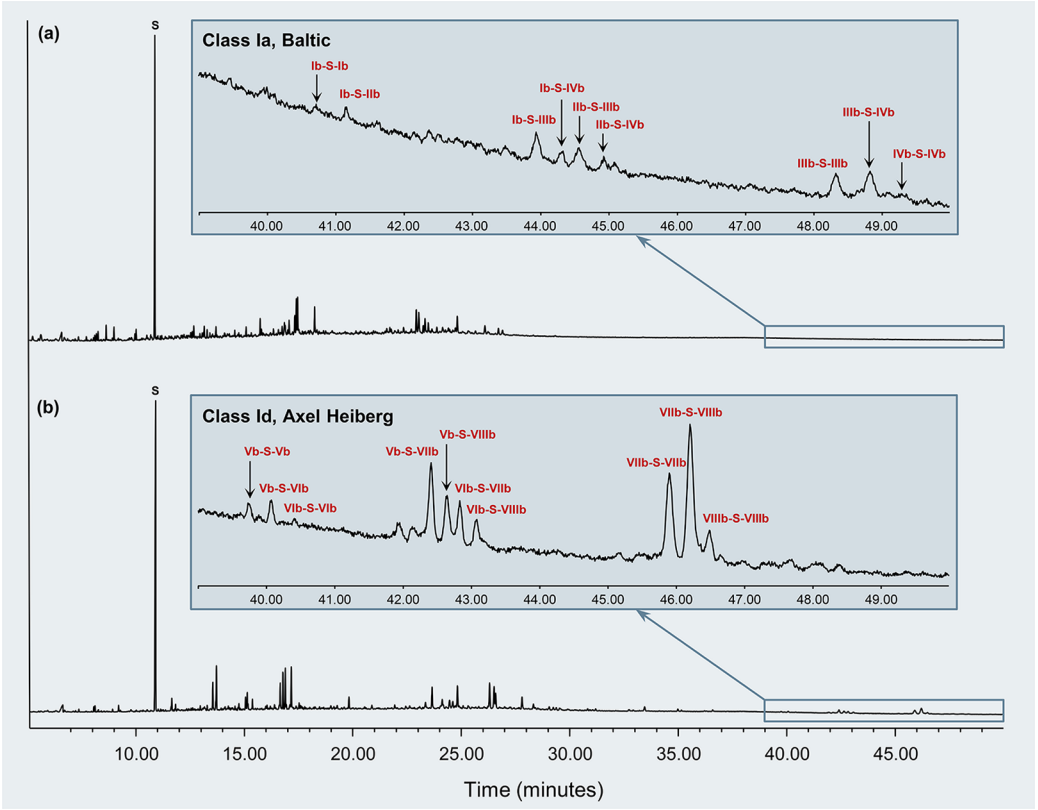

Figure 5. Chromatograms of Class Ia Baltic resinite (a) and Class Id Axel Heiberg resinite (b) with expansion of the segments between 39 and 50 min to show peaks of the diesterification of succinic acid with communol and ozol pyrolysates, respectively. The labeled peaks correspond to molecular structures described in Figure 6 and mass spectra in Table 1.

thus are the most prominent of the series. The same pattern of succinate diester combinations is seen in Figure 4b for the enantio Class Id compounds. Once again, the regular succinate diesters elute at retention times that are offset from the enantio compounds.

The mass spectra and elution pattern of the 10 peaks indicated combinations of similar compounds with varying molecular mass. It was the molecular ion and characteristic fragment ions that most strongly indicated that the compounds were combinations of communol and ozol pyrolysate compounds with a succinyl cross-linkage. Characteristic ions for the diesters are provided in Table 1. As in the case of the monoesters, these fragment ions are formed through elimination of the methyl group at the junction of the A/B rings followed by dehydrogenation and cleavage of the C−O bond at the succinate group (Figure 6).[28] In contrast to compounds Ib-S to VIIIb-S in Figure 3, the mass spectra of these compounds do not contain the m/z 73 ion and thus have not been derivatized by HMDS. Diester succinates composed of combinations of compounds Ib and IIb (Figure 5a) and Vb, and VIb (Figure 5b) had $M^{+\bullet}$ of m/z 498 and eluted in the first cluster of peaks. They were identified based on the order of elution of nonsuccinylated compounds in Figure 2 and the relatively greater abundance of the peaks labeled Ib-S-IIB and Vb-S-VIb, which actually contain both possible combinations, i.e., Ib-S-IIb and IIb-S-Ib. Characteristic fragment ions for these three compounds include m/z 175 and m/z 190, which are also prominent in the mass spectra of related compounds in Figures 2 and 3. Compound IIb-S-IIb contains the least abundant communol pyrolysate (IIb) and it is not resolved from the baseline, but the corresponding enantio compound (VIb-S-VIb) is labeled in Figure 5b. The middle cluster of four peaks contains diester succinates composed of combinations of Ib or IIb with IIIb or IVb (Figure 5a) and Vb or VIb with VIIb or VIIIb (Figure 5b). The identification of the peaks was elucidated from the molecular ions (m/z 512, 510, 512, and 510) and the order of elution of the corresponding pyrolysates in Figure 2. Characteristic fragment ions in the mass spectra include m/z 175, 189, 190, and 204 for those diesters containing Ib or IIb and IIIb (Figure 4a) and Vb or VIb and VIIb (Figure 4b), and m/z 175, 187, 190, and 202 for those diesters containing Ib or IIb and IVb (Figure 4a) and Vb or VIb and VIIIb (Figure 4b). The final cluster of three peaks includes diester succinates composed of combinations of IIIb and IVb (Figure 4a) and VIIb and VIIIb (Figure 4b). The identification of the peaks was elucidated from the molecular ions (m/z 526, 524, and 522) and the order of elution of corresponding pyrolysates in Figure 2. Again, the central peak of the cluster is more abundant because it contains twice as many diester combinations: IIIb-S-IVb and IVb-S-IIIb (Figure 5a) and VIIb-S-VIIIb and VIIIb-S-VIIb (Figure 5b). Characteristic fragment ions for the three peaks include m/z 189 and 204 for those diesters containing only IIIb or Vb pyrolysates, m/z 187 and 202 for those containing only IVb and VIIIb pyrolysates. All four ions are present in the mass spectra of the central peaks. The mass spectra of all diesters containing either IVb or VIIIb consistently show a significantly higher abundance of ions derived from the fragmentation of the IVb and VIIIb portion of the compound (m/z 187 and 202) than those from the fragmentation of the other alcohol pyrolysate (Table 1). The presence of the diester compounds in the chromatograms shown in Figure 5 is the first direct molecular evidence for the

dx.doi.org/10.1021/ac501073k | Anal. Chem. 2014, 86, 7428−7435

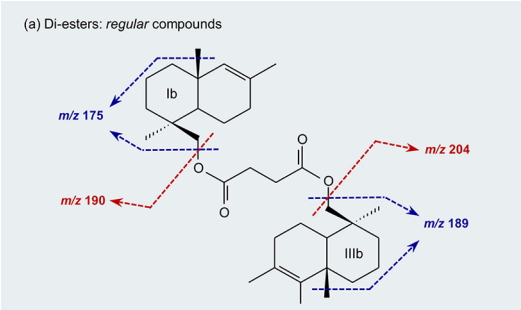

Compounds	Characteristic ions (*m/z*)
Ib-S-Ib	175, 190
Ib-S-IIb	175, 190
IIb-S-IIb	175, 190
Ib-S-IIIb (shown)	175, 189, 190, 204
Ib-S-IVb	175, 189, 190, 204
IIb-S-IIIb	175, 187, 190, 202
IIb-S-IVb	175, 187, 190, 202
IIIb-S-IIIb	189, 204
IIIb-S-IVb	187, 189, 202, 204
IVb-S-IVb	187, 202

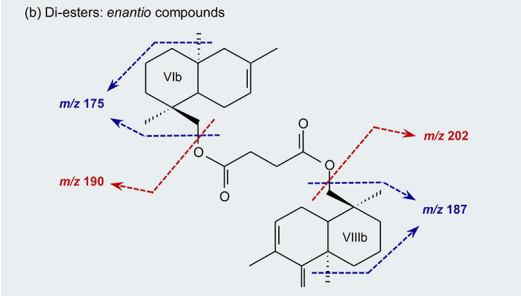

Compounds	Characteristic ions (*m/z*)
Vb-S-Vb	175, 190
Vb-S-VIb	175, 190
VIb-S-VIb	175, 190
Vb-S-VIIb	175, 189, 190, 204
Vb-S-VIIIb	175, 189, 190, 204
VIb-S-VIIb	175, 187, 190, 202
VI-S-VIIIb (shown)	175, 187, 190, 202
VIIb-S-VIIb	189, 204
VIIb-S-VIIIb	187, 189, 202, 204
VIIIb-S-VIIIb	187, 202

Figure 6. Key fragmentations and resulting ions of the diester compounds for the Class Ia resinite (a) and Class Id resinite (b).

cross-linking of alcohol labdanoid moieties in Class I resinite by succinic acid.

Succinic Acid Esterification: Dehydroabietol. Succinic acid is multifunctional within Class Ia and Class Id resinites. In addition to cross-linking the macromolecular structure, it has also been found to esterify with monoterpene alcohols, including borneol, isoborneol and fenchol, and the diterpene dehydroabietol.[12,29−31] In Figure 7, a set of four late-eluting peaks in the chromatogram of the Class Id Canadian resinite sample show that succinic acid connects diterpene alcohols directly to the macromolecular structure. These compounds are tentatively identified as diesters composed of dehydroabietyl succinate esterified to the four ozol pyrolysate compounds Vb−VIIIb (Vb-S-DHAol, VI-S-DHAol, VIIb-S-DHAol, and VIIIb-S-DHAol). A labeled peak at 33.5 min marks the trimethylsilyl ester of dehydroabietyl succinate (DHAol-S), presumably detached from the main polymer through pyrolysis as was similarly seen for the monoester compounds in Figure 3.

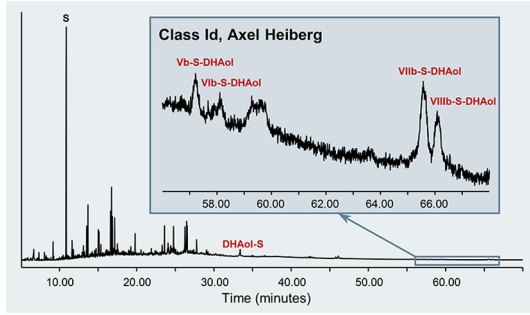

Figure 7. Chromatograms of Class Id Axel Heiberg resinite with expansion of the segment between 56 and 68 min to show peaks of the esterification of dehydroabietyl succinate with ozol pyrolysates Vb−VIIIb. The labeled peaks correspond to molecular structures described in Figure 8 and mass spectra listed in Table 1.

The regular counterparts to these dehydrobietyl succinate compounds were not detected in the Class Ia resinite sample. This is likely due to the relatively greater abundance of ozol and dehydroabietol units within the macromolecular structure of the Class Id resinite. The identification of the peaks is tentative as the molecular ions (*m/z* 576, 576, 590, and 588) are not present in the mass spectra. However, the peaks contain characteristic fragment ions present in previously described Vb−VIIIb compounds, in addition to fragments that are characteristic of dehydroabietol. In the mass spectra, two main ion fragments are formed from the dehydrobietyl group following reaction pathways that include the loss of the methyl group at the junction of the A/B rings, dehydrogenation and cleavage of the C−O bond at the succinate group, yielding the *m/z* 268 and 253 ions, respectively (Figure 8).[28] A third

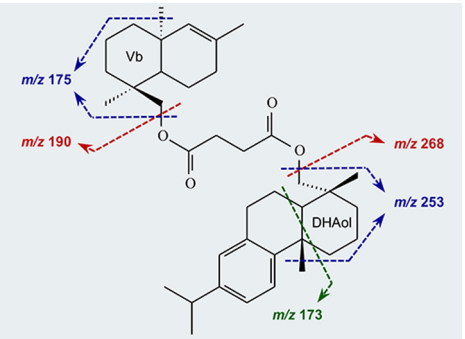

Compounds	Characteristic ions (*m/z*)
Vb-S-DHAol (shown)	173, 175, 190, 253, 268
VIb-S-DHAol	173, 175, 190, 253, 268
VIIb-S-DHAol	173, 189, 204, 253, 268
VIIIb-S-DHAol	173, 187, 202, 253, 268

Figure 8. Key fragmentations and resulting ions of the dehydroabietyl ozyl succinate compounds for the Class Id resinite.

important fragmentation reaction involves the cleavage and rearrangement of the A/B rings yielding the *m/z* 173 ion.[28] The joining of the bicyclic labdane alcohols with the abietane alcohol is made through succinate diester linkage and shows for the first time that nonpolymerized diterpenes are not only occluded, but contribute structurally to the macromolecular structure of Class Id resinite.

dx.doi.org/10.1021/ac501073k | *Anal. Chem.* 2014, 86, 7428−7435

CONCLUSION

After decades of reasonable hypotheses, this study has provided direct molecular evidence that communol and ozol moieties within the polylabdanoid macromolecular structure of Class Ia and Class Id resinites are cross-linked with succinic acid. It has also been shown for the first time that some nonpolymerized diterpenes play a role in the polymeric structure and are not simply occluded within the matrix. The pyrolysis technique using a thermal separation probe altered what had in past studies been an immediate pyrolysis, to a slower one. This new methodology, combined with the use of a mild derivatization reagent (HMDS), has made a substantial difference in the size and complexity of compounds that were released from the rigid polymer matrix. This advancement in the analysis of Class I resinites is an important development that will help in understanding not only the role of succinic acid with Class Ia and Class Id resinites but also the role of other non-polylabdanoid compounds found in resinites. With the use of thermal separation probe pyrolysis, we are developing a clearer picture of structural cross-linkages inside amber.

AUTHOR INFORMATION

Corresponding Author

*J. Poulin. E-mail: jennifer.poulin@pch.gc.ca.

Notes

The authors declare no competing financial interest.

ACKNOWLEDGMENTS

The authors thank Richard Day and Willow Wight at the Canadian Museum of Nature and Malcolm Back at the Royal Ontario Museum for providing resinite samples. We also thank Marcus Kim at Agilent Technologies for resolutely insisting that the thermal separation probe would be a useful addition for our GC–MS.

REFERENCES

(1) Anderson, K. B. *Geochem. Trans.* **2006**, *7*, 1–9.
(2) Anderson, K. B.; LePage, B. A. In *Amber, Resinite and Fossil Resins*; Anderson, K. B., Crelling, J. C., Eds.; American Chemical Society: Washington, DC, 1995; pp 170–92.
(3) Grimaldi; David, A.; Lillegraven; James, A.; Wampler; Thomas, W.; Bookwalter; Denise; Shedrinsky; Alexander. *Rocky Mt. Geol.* **2000**, *35* (2), 163–204.
(4) Lambert, J. B.; Santiago-Blay, J. A.; Anderson, K. B. *Angew. Chem., Int. Ed.* **2008**, *47*, 9608–16.
(5) Langenheim, J. H. *Plant Resins: Chemistry, Evolution, Ecology, and Ethnobotany*; Timber Press: Portland, OR, 2003; pp 143–195.
(6) Otto, A.; Wilde, V. *Bot. Rev.* **2001**, *67*, 141–238.
(7) Wolfe, A. P.; Tappert, R.; Muehlenbachs, K.; Boudreau, M.; McKellar, R. C.; Basinger, J. F.; Garrett, A. *Proc. R. Soc. B* **2009**, *276*, 3403–3412.
(8) Anderson, K. B.; Winans, R. E.; Botto, R. E. *Org. Geochem.* **1992**, *18*, 829–841.
(9) Anderson, K. B. *Org. Geochem.* **1994**, *21*, 209–212.
(10) Poulin, J.; Helwig, K. *Org. Geochem.* **2012**, *44*, 37–44.
(11) Gough, L. J.; Mills, J. S. *Nature* **1972**, *239*, 527–28.
(12) Mills, J. S.; White, R.; Gough, L. *Chem. Geol.* **1984**, *47*, 15–39.
(13) Beck, C. W. *Appl. Spectrosc. Rev.* **1986**, *22*, 57–110.
(14) Anderson, K. B. In *Amber, Resinite and Fossil Resins*; Anderson, K. B., Crelling, J. C., Eds.; American Chemical Society: Washington, DC, 1995; pp 105–29.
(15) Anderson, K. B.; Winans, R. E. *Anal. Chem.* **1991**, *63*, 2901–2908.
(16) Anderson, K. B.; Botto, R. E. *Org. Geochem.* **1993**, *20*, 1027–38.
(17) Chiavari, G.; Fabbri, D.; Prati, S. *Chromatographia* **2002**, *55*, 611–16.
(18) Colombini, M. P.; Bonaduce, I.; Gautier, G. *Chromatographia* **2003**, *58*, 357–363.
(19) Osete-Cortina, L.; Doménech-Carbó, M. T. *J. Chromatogr. A* **2005**, *1065*, 265–278.
(20) Osete-Cortina, L.; Doménech-Carbó, M. T. *J. Anal. Appl. Pyrolysis* **2006**, *76*, 144–53.
(21) Scalarone, D.; Chiantore, O. In *Organic Mass Spectrometry in Art and Archaeology*; Colombini, M. P., Modugno, F., Eds.; John Wiley & Sons, Ltd.: Chichester, West Sussex, 2009; pp 327–361.
(22) Ribechini, E.; Bacchiocchi, M.; Deviese, T.; Colombini, M. P. *J. Anal. Appl. Pyrolysis* **2011**, *91*, 219–223.
(23) McIver, E. E.; Basinger, J. F. *Ann. Mo. Bot. Gard.* **1999**, *86*, 523–45.
(24) Day, R. G. *Bull. - Geol. Surv. Can.* **1991**, *403*, 99–121.
(25) Anderson, K. B.; Bray, W. *Archaeometry* **2006**, *48*, 633–40.
(26) Bray, P. S.; Anderson, K. B. *Science* **2009**, *326*, 132–34.
(27) Hummel, D. O. *Atlas of Polymer and Plastics Analysis*, 2nd ed., Vol. *2*; Carl Hanser Verlag: Weinheim, Germany, 1988; Part a/I, p 234.
(28) Enzell, C. R.; Wahlberg, I. *Acta Chem. Scand.* **1969**, *23*, 871–891.
(29) Stout, E. C.; Beck, C. W.; Kosmowska-Ceranowicz, B. In *Amber, Resinite and Fossil Resins*; Anderson, K. B., Crelling, J. C., Eds.; American Chemical Society: Washington, DC, 1995; pp 130–148.
(30) Czechowski, F.; Simoneit, B. R. T.; Sachanbinski, M.; Chojcan, J.; Wolowiec, S. *Appl. Geochem.* **1996**, *11*, 811–834.
(31) Yamamoto, S.; Otto, A.; Krumbiegel, G.; Simoneit, B. R. T. *Rev. Palaeobot. Palynol.* **2006**, *140*, 27–49.